



Contents lists available at SciVerse ScienceDirect

Optics & Laser Technology

journal homepage: www.elsevier.com/locate/optlastec

Characterization of coating processes in Moiré Diffraction Gratings for strain measurements

João Eduardo Ribeiro^b, Hernani Lopes^c, João Paulo Carmo^{a,*}

^a University of Minho, Department of Industrial Electronics, Campus Azurém, Guimarães, Portugal

^b Polytechnic Institute of Bragança, Department of Mechanical Technology, Campus Santa Apolónia, Bragança, Portugal

^c Polytechnic Institute of Bragança, Department of Applied Mechanics, Campus Santa Apolónia, Bragança, Portugal

ARTICLE INFO

Article history:
Received 12 April 2012
Received in revised form
1 September 2012
Accepted 5 September 2012

Keywords:
Optical techniques
Moiré interferometry
Moiré Diffraction Gratings (MDGs)
replication

ABSTRACT

This paper analyses the influence of the coating process in the optical efficiency of replicated Moiré Diffraction Gratings (MDGs), which are applied on real field applications for measuring both the surface displacements and strains. The Moiré diffraction technique is an experimental full-field, non-contact and high resolution optical method, which can reveal to be very useful in extreme harsh environments. The optical efficiency of the replicated MDGs plays an important role in the quality of the experimental measurements. Two processes were used to obtain the metallic coatings: sputtering and aluminum vaporization. A good coatings quality with high optical efficiency was achieved for both processes (e.g., 17%–28%). However, for the replicated gratings a slight decrease in the optical efficiency was found (e.g., 14%–21%). The MDGs were successfully used for the experimental measurements of displacement and strains in a single lap joint. The measurements also showed that high quality of measurements allowed the identification of unbounded regions.

© 2012 Elsevier Ltd. All rights reserved.

1. Introduction

Nowadays, the emergence of new materials whose mechanical behavior must be characterized has forced the development of new and more adapted measurement techniques [1,2]. In last few years, the optical methods have been used by the industrial and scientific communities as an important measurement technique [3,4], motivate by their high resolution, non-contact and full-field measurements. This is the case of Moiré interferometry, which is used in many optoelectronic applications to measure displacements [5], evaluating deformations within microelectronics devices [6–8], and in optical communications [9,10]. Lithographic and Microsystems specific techniques [11,12] can be used to replicate high-quality Moiré Diffraction Gratings (MDGs) into the surface whose displacements has to be measured.

The Moiré is an experimental technique which allows measuring surface displacements and strains. This is based on the interference fringes resulting from the superposition of two gratings, where one is recorded on the surface specimen and the other is used as a master grating and works as reference. Moiré methods can be used to measure in-plane [13] and out-of-plane [14] components of the surface deformation. For in-plane measurements the Moiré grating must be copied on to the object

surface to interfere with a master grating. The grating on the object surface is deformed by an application of external load. The superposition of deformed and master gratings will produce Moiré patterns or Moiré fringes. For out-of-plane measurements is used the superimposition of a master grating and its own shadow [15,16]. The shadow Moiré fringes are points of equal deformation. The sensitivity difference between the shadow Moiré and the holographic interferometry is further than two orders of deformation magnitude [17]. However, the sensitivity of the shadow Moiré can be improved by the application of optical/digital fringe multiplication techniques [18] and phase-shifting techniques [19].

The main contribution of this paper is related to the analysis of the influence of coating fabrication processes of MDGs in real-time strain measurements and real-field environments.

2. Moiré Diffraction Gratings and technology

The Moiré interferometry is an optical technique that uses the diffraction of coherent light principle produced by a high frequency diffraction grating for measuring the full-field displacements and strain on the object surface [20]. The application of this technique requires the imprinting of gratings into an object surface and at the same time, it should present optical efficiency and a good grating quality. For in-plane measurements, a secondary interference fringes must be created in order to measure the object surface deformation.

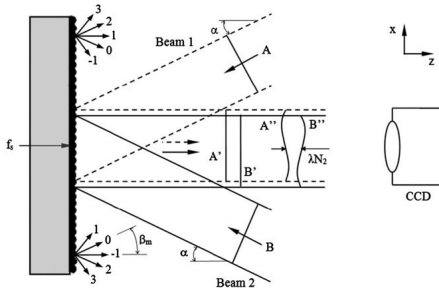


Fig. 1. A schematic representation of the Moiré interferometry principle [21].

A grating divides the incident coherent light into several diffracted wave-trains of smaller intensities. These wave-trains emerge in a given preferred direction (called diffraction orders). Fig. 1 presents schematic representation of the Moiré interferometry principle.

The angles of diffraction are determined by the grating according to the following equation [22]:

$$\sin(\beta_m) = \sin(\alpha) + m\lambda f_s \quad (1)$$

where m is the diffraction order, f_s [lines mm^{-1}] is the specimen grating frequency, α [rad] is the angle of incidence, β_m [rad] is the angle of the m th diffraction order, and λ [m] is the wavelength of the laser light. The first order diffracted beam will interfere with the virtual grating, resulting in the creation of an interferometric pattern which is created by the interference between the two incident beams and has a frequency f that is a double of specimen grating frequency (f_s).

The application of diffraction grating on the object surface, where it is intended to measure the in-plane response, can be performed by two different ways [23]. One is the direct projection of the virtual grating onto the object surface, whereas the other is using a replicate gratings that were previously applied in a mold (master grating). The first can only be applied on small objects that are easily handled. However, the most common and flexible technique is the replication the grating from a mold. The grating mold can be obtained by two different processes by mechanically ruled [24], made by burnishing grooves individually with a diamond tool against a coating of evaporated metal applied to a plane or concave surface, or by holographic process [25].

The holographic method involves the recording of an interference fringe field. This interference field is obtained as a result of two wave fronts on photosensitive polymers (designated by photoresist or PR). In this process, a glass plate with a very low roughness (typically smaller than $\lambda/5$) is coated with a very thin layer of photoresist and is exposed to a virtual grating of frequency $f/2$. This virtual grating is created with the help of two intersecting collimated laser light beams, using ultraviolet (UV) and blue wavelength light. The interference pattern captured by the plate presents a simple harmonic intensity distribution, assuring that the furrows have a symmetrical profile. The PR is then developed using a specific solvent for this purpose. The solubility of the PR increases on exposure to light, and consequently the resist dissolves quickly in the zones of constructive interference. The schematic process of creating the holographic gratings using PRs is presented in Fig. 2.

The spatial frequency of the gratings could be controlled by the angle of the incident laser beam. Considering the angle θ [rad] as

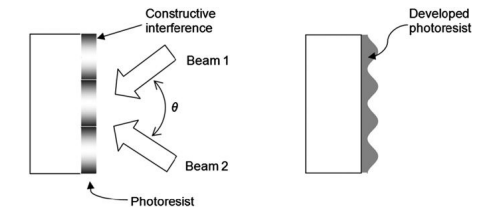


Fig. 2. Holographic grating obtained with PR.

the angle between the two incident beams, the specimen grating frequency, f_s is given by:

$$f_s = \frac{2}{\lambda} \sin(\theta) \quad (2)$$

where λ [m] is the wavelength of the laser light.

The work presented in this paper used this process to pattern the PR. The depth of the PRs' furrow can be optimized by controlling the exposure. Parallel line gratings with 1200 lines/mm were produced with good diffraction efficiencies with respect to the two first-order diffractions. After the creation of the holographic gratings with PR, these must be coated with a thin layer of reflective metal (the most common materials include either the aluminum or the gold). The most usual techniques for coating the gratings are those that make use of the aluminum evaporation and the sputtering. The gratings' mold created by a holographic process is replicated on the specimen surface. Before the replication, the mold is prepared by applying a reflexive metal film above its grating surface. A double coating of aluminum is used, where the first layer is oxidized by allowing air into vacuum chamber and then, a second coating is applied. This second coating is usually preceded by the application of a wetting agent, just after the application of the first layer. The replication of grating is achieved with the help of an adhesive placed between the grating's mold and the specimen's surface. The mold is pried off after the polymerization of the adhesive, leaving a reflective diffraction grating bonded to the surface of the specimen. It must be noted that a weakest interface occurs between the mold and the metal film, which accounts for the transfer of the reflective film to the specimen.

3. Experimental procedure

3.1. Preliminary considerations

One of the most critical factors affecting the efficiency of replicated gratings is the reflexive quality of metal coatings. This factor depends on the coating technique, the material and the thickness of layer. In this paper, two of most common processes for coating the gratings are analyzed: the aluminum evaporation and the sputtering. The efficiency of the gratings are presented, considering few combinations of several factors. These factors include the materials and the thickness of the layers. With respect to the material, layers made of aluminum were obtained by evaporation and by sputtering; layers made of gold were also obtained using the sputtering technique. A set of eight samples were prepared and coated by these two different techniques. Different thicknesses with different coating materials were also obtained. It must be noted that the process to obtain the gratings mold was the same for the eight samples.

The gratings molds developed and presented in this paper were crossed line gratings with 1200 lines/mm. After coating the grating's mold, these were replicated on the specimen surface, which consisted on a steel plate with a roughness R_a of 2.1 μm .

* Corresponding author. Tel.: +351 253 510190; fax: +351 253 510189.
E-mail address: jcarmo@dei.uminho.pt (J. Paulo Carmo).

The replication of gratings must be performed carefully to maintain the reflection quality of grating in the whole area. The diffraction efficiencies of gratings were measured before and after the replication. The comparison of results was further done.

3.2. MDG fabrication process

It was pursued the goal to achieve good procedures (whose definition includes high-yield and high-reproducibility) for obtaining the best possible diffraction efficiencies in each of the two first-order diffractions (e.g., +1 and -1). In the first place, it was used the most common method and material for coating the gratings: the application of aluminum with the help of the evaporation technique. This procedure was followed for the first two samples, but the results weren't very good and it was tried an alternative technique, the sputtering. Two mold grating samples (3 and 4) were coated with aluminum, using the sputtering, but, unfortunately, the results were even worse than the former. Meanwhile, it was verified that few parameters in the evaporation aluminum technique could be changed. This change of evaporation parameters allows better results compared with the first two samples. In this sequence, three more samples (5, 6 and 7) were prepared with satisfactory results. With respect to the samples 1 and 2, the gratings were coated with two layers of aluminum using the evaporation process. Between the two layers was applied a wetting agent (Kodak PhotoFlo®). Table 1 lists the thickness of each layer.

The coating of the sample 1 seems to be the most uniform of all. However, this uniformity has the cost to present a dark color and a low reflectivity. The sample 2 was less uniform, showing areas with a very bad appearance, while the others presented a good quality and strong reflection. The gratings of the samples 3 and 4 were coated with two layers of aluminum using the sputtering process. The wetting agent was applied on first layer. The first aluminum layer presented a thickness of 10 nm, whereas the second layers presented a thickness of 20 nm and 40 nm for thickness of the samples 3 and 4, respectively. The samples 5, 6 and 7 were coated with aluminum deposited by evaporation. In this case, two coatings were also used. The thicknesses of these three layers are also listed in the Table 1.

The coating of sample 5 presented a low reflection coefficient, so this sample was not replicated in any specimen. The samples 6 and 7 presented a much high reflection, although the sample 7 presented a region whose reflection was smaller than the rest of the sample surface. The last sample (the number eighth) was fabricated for testing a different reflexive material, e.g., the gold. The sputtering process was used to coat the diffraction grating of the sample. For this case, the first layer had 10 nm and the second 30 nm. The obtained results showed that few areas of the coating had good quality; however it was very isolated and small. Therefore, this makes this sample inadequate for using in any measurement.

3.3. MDG replication

The grating replication has the objective of recording the diffraction grating on specimen's surface. The replication is carried

Table 1
The layers thickness on the gratings.

Sample number	First layer (nm)	Second layer (nm)
Sample 1	20	60
Sample 2	40	40
Sample 3	10	20
Sample 4	10	40
Sample 5	30	30
Sample 6	30	50
Sample 7	30	70
Sample 8	10	30

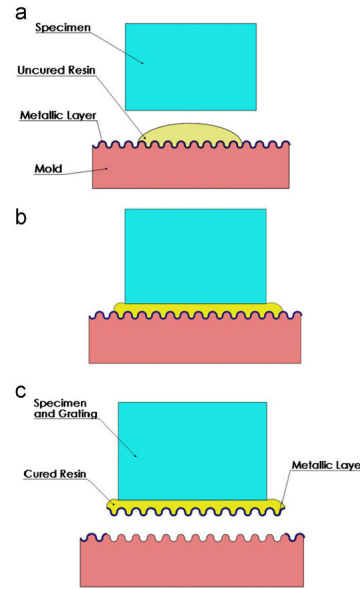


Fig. 3. Main steps to replicate diffraction gratings from mold to specimen.

out from the coated diffraction grating mold, using the procedures which is shown in Fig. 3.

This process of replication was applied for the majority of the samples, where the reflection quality of respective gratings was analyzed. To compare the obtained results, the replication was executed on specimens of steel with the same geometry, dimensions and surface finishing ($R_a=2.1\ \mu\text{m}$). These steel specimens have a length of 20 mm, width of 25 mm and thickness of 5 mm.

Comparing the replication of the samples 1 and 2, it was possible to observe for the first one that the coating of replicated grating had a low quality (ripples and fractures), low reflectivity of the replicated grating and difficulty in the diffraction of light on the replicated grating. On the other hand, on the sample 2 the coating of replicated grating varied among areas of low (but better than in sample 1) and acceptable quality. The refraction index of the replicated grating, varied with its region between small and high values. Finally, the diffraction of the light on the replicated grating was interspersed between areas of good diffraction and others with low-diffraction.

After analyzing the replication of samples 3 and 4, it was possible to verify that the sputtering process leads to a very high adherence of aluminum layers. The process of dried off was difficult, the diffraction grating transfer of sample 3 was not uniform, causing regions with good transfer and others where there was no any transfer of aluminum layer occurred.

It was impossible to replicate grating in the sample 4 because the aluminum layer was strongly glued on it. For the specific case of the sample 6 it is possible to note that the substrate reacted with the aluminum coating layer, whose consequence was the rising of a very dark and opaque gratings. This reaction has occurred possibly due to the excessive dust that existed on the area of epoxy grating.

Table 2
The measurement of the first order diffracted beam power, before and after the replication of grating.

	Before grating replication (mW)	After grating replication (mW)
Sample 1	17.26	14.38
Sample 2	18.57	17.28
Sample 3	15.41	14.75
Sample 4	18.33	NR*
Sample 5	16.97	15.77
Sample 6	21.43	20.02
Sample 7	22.51	21.39
Sample 8	27.96	NR*

* No replication.

The sample 7 is very similar to the sample 5, presenting a more uniform coating. However, the sample 7 had a better quality of gratings than the others samples. This was verified by the good diffraction efficiency.

For the sample 8, it was impossible to replicate the grating mold with a gold coating, because it was strongly glued on the sample, a similar phenomenon happened with the sample 4. These observations lead to the conclusion that the sputtering process is not suitable to these applications.

3.4. Light power measurement

It is required the measurement of the powers from both the direct laser and diffracted beams to obtain the diffraction efficiency. To measure the power of beams was used a Laser Power Meter model PM121D and a 2-W laser (from Coherent, Verdi). The laser source used for doing the measurements presented a wavelength of 532 nm and had a power of 100 mW. The power measurements of the first order diffracted beam light in each grating (before and after replication) are indicated in Table 2. The given values were measured on the highest diffractions regions of the gratings. The measured power of directed beam light for the laser source was 100 mW.

4. Assessment of diffraction efficiency

The efficiency of a reflection grating is defined as the energy flow (power) of monochromatic light diffracted into the order being measured. This can be made relative either to the energy flow of the incident light (absolute efficiency) or to the energy flow of specular reflection from a polished mirror substrate coated with the same material (relative efficiency) [26]. The following equation presents the definition of the absolute efficiency used in this paper:

$$\text{efficiency} = \frac{\text{diffracted beam power}}{\text{direct beam laser power}} \quad (3)$$

The gratings developed in this work are a very low modulation gratings. These gratings operate in the scalar domain, where the theoretical efficiency peak for sinusoidal grooves is 33.8% [27]. The diffraction beam with the first order (+1 or -1) is the one which must be used for doing the measurements, because in the zero order, the grating acts either as a window or a mirror. For this reason, the absolute efficiency of first order diffraction beam was the only one to be determined. The absolute efficiency is computed for a diffraction angle of 39.7° and a wavelength of 532 nm. Figs. 4 and 5 represent the absolute efficiency for the coated gratings before and after their replication, respectively.

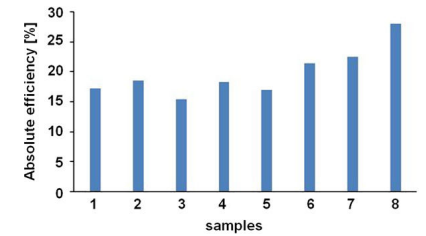


Fig. 4. Absolute efficiency on the coated gratings, before the replication.

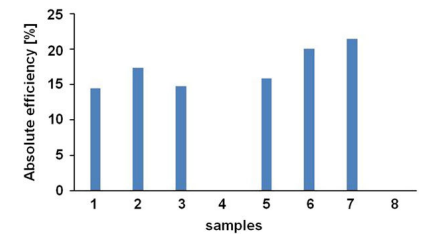


Fig. 5. Absolute efficiency on the coated gratings, after the replication.

The best absolute efficiency was obtained on the gold coating. The efficiency of samples 6 and 7 are also acceptable for measurement applications.

It is possible to verify that the efficiency decrease after the replication. Some of mold gratings could not be replicated.

5. Case-study

Adhesives are increasingly being used to replace traditional fastening methods in industrial applications, such as welding, bolts and rivets. In cars and other transport applications (where the weight reduction plays a key factor in new developments) has led to the rapid expansion of adhesives. The adhesives can be used for bonding different kind of materials, including ceramics, metals, glass, plastics and composites. Their main advantages are the distribution of loads across the entire joint area, excellent fatigue properties, attenuation of mechanical vibrations and noise, sealant functions, reduction in galvanic corrosion between dissimilar metals, and a faster and more cost-effective assembly method. However, their resistance is highly affected by the presence of unbonded regions. The goal of this paper is presenting an experimental technique to find detached regions in a single lap joint by measuring both the in-plane displacements and the strain fields. To achieve this objective, an experimental technique based on Moiré Interferometry Technique (MIT) is proposed. This requires the development of techniques for the replication onto the specimen's surfaces gratings with high quality diffraction. The analysis was performed in the specimen presented in Fig. 6.

The single lap joint was composed of two adherents and a thin adhesive layer (see the photography in Fig. 6). The material used as an adherent was an aluminum alloy (1050 alloy), whereas the material used as an adhesive was an epoxy (Araldite, Standard Ceys, Reference 3148515/00). A 100 N load was applied in the single lap joint specimen for analyzing both the variation of displacement and strain field within the surface of the specimen and the influence of the unbonded region. For that purpose was

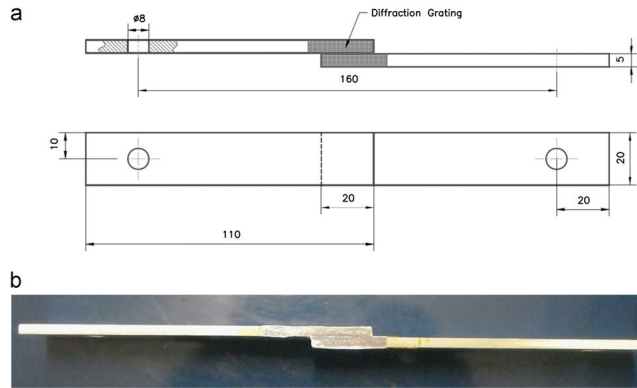


Fig. 6. (a) The geometry of the single lap joint specimen used in this analysis (all distances are expressed in millimeters), (b) A photograph of the single lap joint specimen.

developed a load system to apply a load into the specimen. Moreover, it was used an optical set-up for Moiré interferometry to analyze and measure the in-plane displacement field caused by the applied load. Fig. 7 illustrates a schematic of the used optical set-up. In this figure, LA is the laser source, Ms is a mask, C is the collimator, WM is a window mask, CB is the collimated beam, M1, M2, M3 and M4 are plane mirrors, PP is a parallel plate glass, L is a lens, SLJ is the single lap joint specimen, DG is the diffraction grating, LM is the load mechanism and I is the interferometer. It was also used a four-beam optical system to produce displacement fringe patterns in *u* and *v* directions. The collimated laser beam is partially obstructed by the window mask. This is constituted by three elements whose function is to illuminate simultaneously the grating and the mirrors as follows: illuminating M2 and the grating by opening the middle element allows the measurement of the displacement in the *u* direction; otherwise illuminating M3 and M4 by opening the upper and down elements the measurement of displacement is done in the *v* direction.

The light source used in the set-up was a 2 W laser from Coherent (Verdi). A CCD camera, Sony model XC-8500CE (with a resolution of 782 × 582 pixels) was used for allowing the acquisition of images. A high frequency grating previously replicated on the lap joint surface (see Fig. 6) was also used. The used grating consisted on a crossed 1200 lines/mm, which was obtained by aluminum vaporization on the top of an epoxy replication of a master grating. The procedures and parameters for obtaining these grating were the same described for the sample 7. The replication process was already described in this paper. The setup proposed by Czarnek [28] was used in the virtual grating generation by means of laser interferometry, where the incident angle, α , is 39.7°. Fig. 7 shows a schematic representation of the measurement setup, as well as the photographs of the experimental test. The reference images were recorded after super-positioning the virtual grating over the object replication grating. Then, it was applied a load of 100 N for producing the moiré fringes in result of the displacements. After obtaining these fringes, they recorded with the help of the camera. A tiltable parallel glass plate was used to promote phase modulation, in order to perform a four image phase calculation algorithm [29]. The phase modulation was created by tilting parallel glass plate (PP), mounted in front of the CCD camera (see Fig. 7).

The four-point technique was used in this paper for performing the phase modulations: This technique uses four intensities

values with different phase shifts, but with relative shifts of $\pi/2$ rad steps. It is written in the form

$$\varphi = \arctan \left(\frac{I_4 - I_2}{I_1 - I_3} \right) \quad (4)$$

where I_1, I_2, I_3 and I_4 are intensities recorded in the detector for four different interferograms with phase shifts of $\alpha = 0, \pi/2, \pi$ and $3\pi/2$ [rad]. Analyzing the eq. (4), it is possible to verify the existence of discontinuities for the phase values of π and $-\pi$ [rad], whose values result from the $\arctan(\dots)$ function. These discontinuities are eliminated by using algorithms developed for this purpose (e.g., unwrapping). Thus, the absolute phase maps can be computed by phase unwrapping to reveal the accurate displacement field. For this purpose, it was created an artificial unbonded region in the single lap joint specimen to study the influence of that damage in the displacement and strain field variation. The specimen was mounting into the load system (as showed in Fig. 7), being followed by the load application. After the load application, four phase maps were recorded for each orthogonal direction with phase shifts steps of $\pi/2$ [rad] [30]. The phase steps are created by tilting the parallel plate (PP in Fig. 7). The obtained phase maps were used to measure the displacement field on the adhesive joint.

Figs. 8 and 9 represent the four images in the two orthogonal directions (*u* and *v*) for doing the phase modulation. The analysis of the adhesive joint was done in a region near the end of the board, because the highest stress value occurs in this region. Therefore, the risk of collapse is maximum in this region. Typically, this is the location where the rupture starts.

The post-processing to obtain the displacement field used image processing algorithms, which mainly consisted on filtering, phase calculation and unwrapping and spatial differentiation. The displacements fields are obtained by filtering and unwrapping the phase maps. The displacement fields for two orthogonal directions, which are usually called *u* and *v* directions, are presented in Fig. 10. In this figure, the ordinate axis represents the thickness of the single lap joint, while the abscissa axis represents the length of the analyzed region.

The unbonded region is classified as damage in the adhesive. There are different methods for detection and evaluation of damage, but the most important are based on the measurement of the rotation fields and the strain field gradients [23]. It was applied the strain field gradients method in this case-study, whose values were computed by way of the differentiation algorithm. This

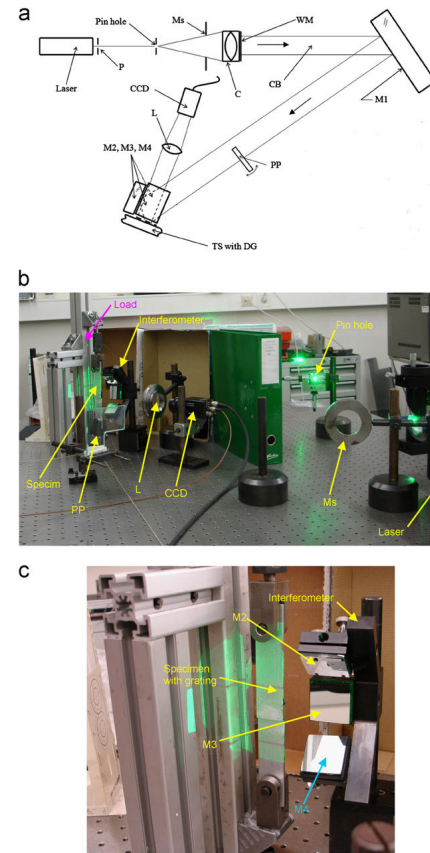


Fig. 7. (a) A schematic presentation of the Moiré interferometry optical set-up [30] used and (b) respective photograph. (c) A detailed view of the specimen mounted for doing the measurement.

algorithm was implemented in this paper and at the same time, it differentiates the displacement field measured by Moiré interferometer technique.

Differentiation algorithms were used to assess the strain field gradients [24]. Fig. 11 shows the strain field gradient for *u* direction, where it is possible to observe the unbonded region.

The value of the strain in the unbonded region is higher than in the other regions of the specimen, which allow to conclude that this region is weaker and probably will suffer rupture before happening the maximum stress of this joint.

6. Conclusions

The experimental results showed that metallic coatings obtained with the sputtering process can be classified as acceptable or good. Nonetheless, these coatings are very difficult to

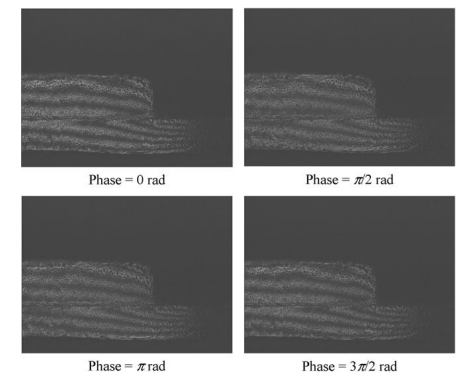


Fig. 8. Fringe pattern for the component of displacement in *u* direction, caused by a load of 100 N.

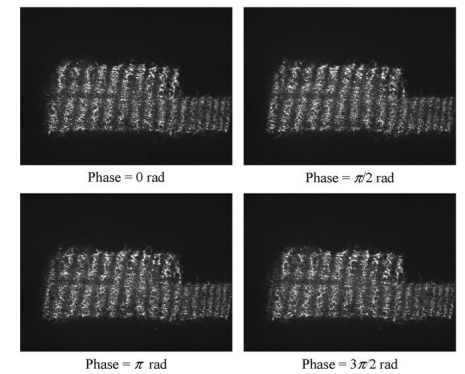


Fig. 9. Fringe pattern for the component of displacement in *v* direction, caused by a load of 100 N.

replicate because they stay strongly glued onto the substrate (e.g., the mold gratings). On the other hand and fortunately, the aluminum vaporization process allows the fabrication of metallic coatings with a high reflection index if the second layer is thick (i.e., more than 60 nm), thus making this process suitable for replicating the gratings. It is very important to control the cleanliness of the environment because any dust particle can result on opaque surfaces which difficult the light reflection.

The efficiency before the replication was measured within the range between 17% and 28%. Additionally, the efficiency after the replication was measured between 14% and 21%. It is possible to conclude that the efficiency decreases after the replication process. However, the values of the efficiency were suitable enough for optical measurement and control applications. For future works is important to improve the replication process to achieve a better efficiency.

The Moiré interferometer technique can be used to measure the displacement field (*u, v*) in single lap joints with a very good resolution. The strain fields obtained by numerical differentiation allows successfully identification of the unbonded region that

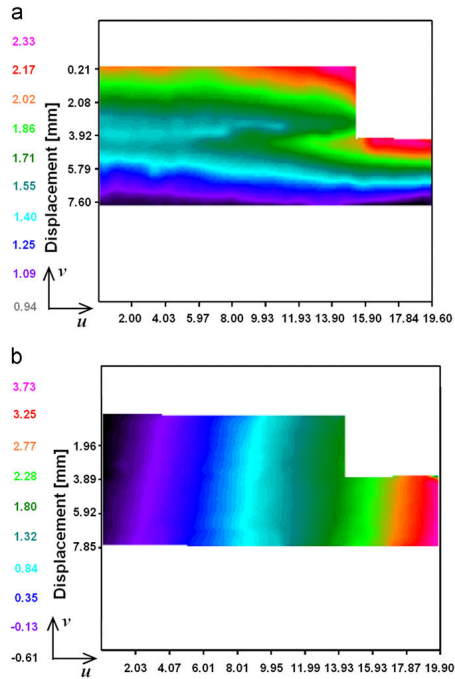


Fig. 10. Displacement field of the single lap joint on the analyzed region, (a) in the u direction and (b) in the v direction, obtained with Moiré interferometry. The displacements units are in millimeters.

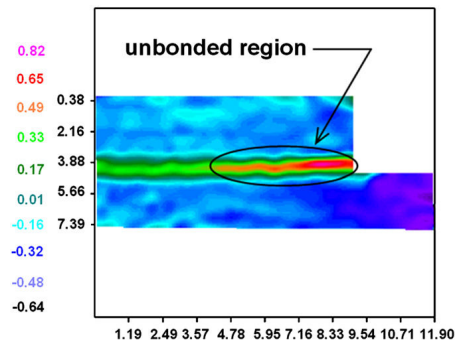


Fig. 11. The detection of unbonded region using the Moiré interferometry technique. The strain units are expressed in microstrains.

was artificially created. The good quality of the results makes this experimental technique a very interesting alternative for the detection of unbonded regions for this kind of joints.

Acknowledgments

This work was fully supported by the Portuguese Foundation for the Science and Technology (FCT) under the financial Grant FCOMP-01-0124-FEDER-010236, through Project Ref. FCT/PTDC/EME-PME/102095/2008.

References

- [1] Botsis J, Humbert L, Colpo F, Giaccari P. Embedded fiber Bragg grating sensor for internal strain measurements in polymeric materials. *Optics and Lasers in Engineering* 2005;43:491.
- [2] Wronkowski L. Diffraction model of an optoelectronic displacement measuring transducer. *Optics and Laser Technology* 1995;27:81.
- [3] Murukeshan VM, Keong N, Krishnakumar V, Seng O, Asundi A. Double shearography for engineering metrology: optical and digital approach. *Optics and Laser Technology* 2001;33:325.
- [4] Lee J, Molimard J, Vautrin A, Surrel Y. Diffraction grating interferometers for mechanical characterizations of advanced fabric laminates. *Optics and Laser Technology* 2006;38:51.
- [5] Xie H, Shang H, Dai F, Li B, Xing Y. Phase shifting SEM moiré method. *Optics and Laser Technology* 2004;36:291.
- [6] Liu Z, Lou X, Gao J. Deformation analysis of MEMS structures by modified digital moiré methods. *Optics and Lasers in Engineering* 2010;48:1067.
- [7] Ifju P, Han B. Recent applications of Moiré interferometry. *Experimental Mechanics* 2010;50:1129.
- [8] Chen L, Cooper D, Smith P. Transmission filters with multiple flattened passbands based on chirped moiré gratings. *IEEE Photonics Technology Letters* 1998;10:1283.
- [9] Chen L, Smith P. Demonstration of incoherent wavelength-encoding/time-spreading optical CDMA using chirped moiré gratings. *IEEE Photonics Technology Letters* 2000;12:1281.
- [10] Kärkkäinen A, et al. Direct photolithographic deforming of organomodified siloxane films for micro-optics fabrication. *Applied Optics* 2002;41:3988.
- [11] Li Y, Xie H, Guo B, Luo Q, Gu C, Xu M. Fabrication of high-frequency moiré gratings for microscopic deformation measurement using focused ion beam milling. *Journal of Micromechanics and Microengineering* 2010;20:1.
- [12] Burch JM. Moiré fringe technology. *Optics and Laser Technology* 1972;4(5):248.
- [13] Reid G, Rixon R, Messer H. Absolute and comparative measurements of three-dimensional shape by phase measuring moiré topography. *Optics and Laser Technology* 1984;16(6):315.
- [14] Takasaki H. Moiré topology. *Applied Optics* 1970;9(6):1457.
- [15] Takasaki H. Moiré topology. *Applied Optics* 1973;12(4):845.
- [16] Weissman EM. Experimental tire mechanics by Moiré. *Optics and Lasers in Engineering* 1990;13(2):117.
- [17] Han B. Interferometric methods with enhanced sensitivity by optical/digital fringe multiplication. *Applied Optics* 1993;32(25):4713.
- [18] Mauvoisin G, Brémand F, Lagarde A. Three-dimensional shape reconstruction by phase-shifting shadow moiré. *Applied Optics* 1994;33(11):2163.
- [19] Post D, Barakat W. High-sensitivity Moiré interferometry—a simplified approach. *Experimental Mechanics* 1981;21(3):100.
- [20] Post D. Moiré interferometry at VPI and SU. *Experimental Mechanics* 1983;23(2):203.
- [21] Czarnek R. Super high sensitivity Moiré interferometry with optical multiplication. *Optics and Lasers in Engineering* 1990;13:87.
- [22] Ribeiro J, Monteiro J, Vaz M, Lopes H, Piloto P. Measurement of residual stresses with optical techniques. *Journal of Strain: An International Journal for Experimental Mechanics* 2009;45(2):123.
- [23] Gerasimov F, Sergeev V, Telteviskii I, Sergeev V, Marichev B. The use of Moiré interference fringes to control the ruling of diffraction gratings. *Optics and Spectroscopy* 1965;19:152.
- [24] Wadsworth N, Marchant M, Billing B. Real-time observation of in-plane displacements of opaque surfaces. *Optics and Laser Technology* 1973;5(3):119.
- [25] Rayleigh Lord. On the manufacture and theory of diffraction gratings. *Philosophical Magazine Series 4* 1874;47:193.
- [26] Loewen E, Nevière M, Maystre D. Grating efficiency theory as it applies to blazed and holographic gratings. *Applied Optics* 1977;16(10):2711.
- [27] Czarnek R. Three-mirror, four-beam Moiré interferometer and its capacities. *Optics and Lasers in Engineering* 1991;15(2):93.
- [28] Creath K, Schmit J. N-point spatial phase-measurement techniques for non-destructive testing. *Optics and Lasers in Engineering* 1996;24:365.
- [29] Ribeiro J, Monteiro J, Lopes H, Vaz M. Moiré interferometry assessment of residual stress variation in depth on a shot peened surface. *Journal of Strain: An International Journal for Experimental Mechanics* 2011;47(1):e542.
- [30] Lopes H, Santos J, Soares C, Guedes R, Vaz M. A numerical-experimental method for damage location based on rotation fields spatial differentiation. *Computers and Structures* 2011;89(19-20):1754.